from the interface between the materials and the generation of significant electric fields. Depending upon the conditions of the system, this electric field can exceed the dielectric breakdown strength of the materials and cause an electrical discharge which, in turn, can lead to failure of the system.

Although electrification can also occur when two solid materials are in relative motion, this article focuses on systems where one of the materials is a stationary solid and the other is a moving liquid dielectric. As a particular example, transformer oil is commonly pumped through electric power transformers to improve the heat transfer while maintaining the electrical insulation. This allows the transformer to operate at higher power levels. Because of the motion of the liquid, charge separation occurs at the interface of liquid and solid boundaries. With the dielectric electrically insulating and internal components of the apparatus electrically isolated, significant charge can accumulate so that electrical discharges can occur. These discharges reduce the dielectric strength of the insulation and ultimately lead to failure of the transformer.

GENERAL STREAMING ELECTRIFICATION PROCESS

The process of flow or streaming electrification involves four distinct stages: generation, transport, accumulation, and leakage. In the generation stage, chemical reactions in the bulk region of the liquid create positive and negative charged species. In the bulk region, these charged species neutralize one another so that there is no net charge, but at the boundaries between the liquid and the solid phases, one of the charged species is typically preferentially adsorbed onto the interface while the opposite polarity species is diffusely distributed into the liquid. When the liquid is stationary, this equilibrium separation of the charge carriers is called the electrical double layer. When the liquid is in motion, some of the distributed charge from the double layer is entrained by the liquid flow as shown in Fig. 1. This entrained charge is then transported to downstream locations where it can accumulate in the liquid volume or on insulating or isolated surfaces. The charge accumulates until the leakage rate balances the accumulation rate or an electrical discharge occurs.

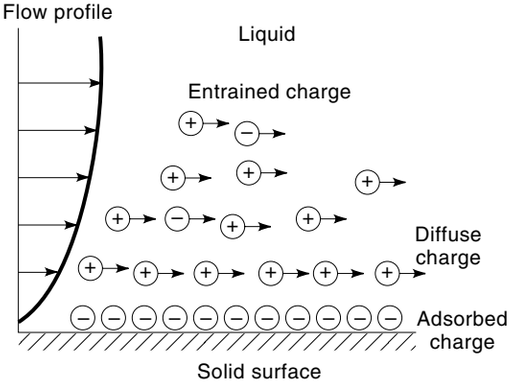

Figure 1. A preferential adsorption of negative ions onto the solid leads to a net positive charge in the liquid which is then entrained in the fluid flow.

STATIC ELECTRIFICATION

Static electrification refers to the development of a net electrical charge by the relative motion between two dissimilar materials. It generally involves the separation of charged species

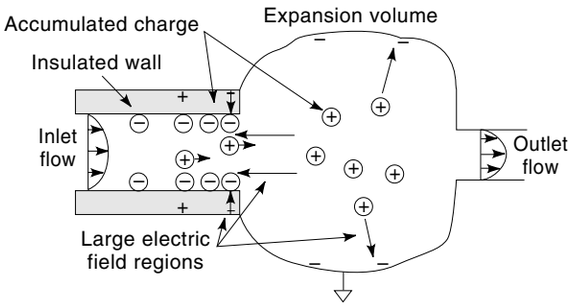

Figure 2. High-velocity liquid flow through narrow passages transports ions downstream and creates large local electric fields.

Figure 2 illustrates the transport and accumulation of charged species from a narrow high flow rate region into an expansion region, as would be the case for fluid flowing into a tank or oil flowing through the windings of a transformer into the header region. Charge can accumulate along the boundaries of the duct region, if the duct is isolated or composed of an insulating material, and in the volume and on the walls of the expansion region. This charge accumulation causes the electric potential to rise and leads to electric fields within the duct wall and between the space charge region in the expansion volume to the enclosure walls or to the opposite polarity charge on the inside surface of the duct. If the electric field in any of these regions exceeds the breakdown strength of the dielectric then an electrical (spark) discharge will occur. The peak electric field and the amount of charge that can accumulate are limited by the leakage through the solid insulation of the ducts and through the volume of the liquid. The characteristic time constant for the volume leakage process in the dielectric liquid is the relaxation time $\tau_e = \epsilon/\sigma$, where ϵ is the dielectric permittivity and σ is the conductivity. The relaxation time indicates that the charge leakage rate is fast for high-conductivity materials and slow for low-conductivity materials. Representative properties for a room temperature hydrocarbon liquid are $\epsilon = 2.2\epsilon_0$, with $\epsilon_0 = 8.854$ pF/m the permittivity of free space, and $\sigma \approx 0.1$ pS/m to 100 pS/m so that $\tau_e \approx 200$ s to 0.2 s. If the residence time of the liquid inside the expansion region is long compared to its dielectric relaxation time then almost all of the charge relaxes to the walls of the expansion region and the liquid exiting the expansion region is essentially uncharged.

The stages of the electrification process are similar to those found in a Van de Graaff generator where an insulating belt transports charge from a corona source to a conducting dome. The charge accumulates on the dome, raising the electrical potential, until the accumulation rate balances the leakage rate to ground or a discharge occurs. However, unlike the Van de Graaff generator, the stages of flow electrification are not necessarily spatially distinct and most factors, such as the temperature, are involved in more than one stage. This coupling of the stages makes it difficult to isolate each of the stages in individual structures, such as pipes, ducts, pumps, and filters. Nevertheless, most structures can be categorized according to their net contribution to the fluid volume charge density as the fluid flows through them, as either a charge generator if the charge density increases or a charge relaxer if the charge density decreases. For example, filters usually act as charge generators because of the large surface area exposed to the flowing fluid. This categorization is useful when trying to understand the role of each component in a flow network but does not necessarily lead to a better understanding of the dynamics occurring inside each structure since the categorization may be influenced by other factors such as the temperature or the contamination level from impurities.

A complete understanding of the electrification processes requires coupling the laws of electromagnetism, fluid mechanics, heat transfer, and electrochemistry and relating these laws to observed critical factors such as the flow rate, temperature, additive concentrations, and energization. More specifically, the generation and recombination of the various charged and neutral species in the liquid volume and at the interface between the liquid and the solid are described by chemical reactions. Since ions from these chemical reactions carry a net charge, the laws of electroquasistatics are necessary to describe the associated electrical potentials and field intensities. The transport of the ions by the liquid flow is described by the laws of fluid mechanics while the heat transfer equations describe the temperature variations throughout the system.

The interdisciplinary nature of processes similar to flow electrification has been explored in detail in several other fields, including physicochemical hydrodynamics and colloid chemistry. Usually the emphasis in these other fields has been on aqueous solutions, where the electrical double layer has a significant effect on the interfacial dynamics and measurements of the bulk properties. Because of the importance of the double layer, the term *electrokinetic phenomena* is conventionally used to describe the interaction of an electric field with the mobile charge in the double layer (1). Electrokinetic phenomena have been classified according to the interfacial material that is moving (the liquid or the solid) and whether the motion is driven by an electric field (electroosmosis, electrophoresis) or an electric field is created by the motion (streaming potential or current). Thus, flow electrification is a subset of electrokinetic phenomena. However, usually when electrification leads to electrical discharges and poses a problem the liquids tend to be nonaqueous rather than aqueous so the results obtained in other fields are not always directly applicable.

ELECTRIFICATION IN INDUSTRY

Several industries involved with the transport or flow of semi-insulating liquids have had to cope with the problems and hazards posed by flow electrification. A review of the critical factors and mitigation techniques shows the commonality between the different applications.

Petroleum Industry

One of the first industries to identify flow electrification as a hazard was the petroleum industry where many of the liquids refined from crude oil are insulating when in a pure state (2,3). The transport of these insulating liquids through pipes and filters and between storage tanks and vehicles allows for significant charge to accumulate in the liquid volume, at the surface between the liquid and vapor spaces, and even on the container walls if the container is not grounded. With the va-

por above the liquid typically combustible, electrostatic discharges of sufficient energy can result in explosions and fires.

Critical factors which affect the electrification hazard are the flow rate, the conductivity, the temperature, and the moisture content of the fluid. Not surprisingly, higher fluid flow rates lead to an increase in the net charge being entrained and transported by the fluid. In contrast, increasing the conductivity leads to competing effects: it increases the number of charged species available for transport by the flowing fluid but also increases the conductivity which decreases the charge relaxation time and the distance that the charge can travel before being neutralized. The net result is that significant charge accumulation only occurs for intermediate conductivities where there is enough charge to be separated by the fluid flow and the relaxation time is large enough for charge to be transported over an appreciable distance. The temperature affects the combustability of the gas vapor and the material properties such as the conductivity and viscosity of the liquid. Water in the fluid generally increases the amount of charge generated by the flow (2,4).

Several techniques have been developed to avoid the electrification hazard. The basic ones involve grounding all of the metallic surfaces to prevent the electric potential from rising above the breakdown strength of the surrounding medium and lowering the flow rate to reduce the charging rate. Antistatic ionizable additives are also added to the fluid to greatly increase the electrical conductivity of the fluid to 50 pS/m to 300 pS/m even when present in trace quantities (mass fractions of order parts per million). Other passive and active techniques involve neutralizing the entrained charge by injecting charge of the opposite polarity into the fluid but these only have limited applicability since there is no guarantee that they reduce the charge under all operating conditions and they require specialized equipment (5).

Electric Power Industry

The increasing demand for electricity has driven the design and construction of electric power apparatus toward compact sizes and operation at higher power levels. This has led to the use of new dielectric materials, changes in the chemical composition of insulating liquids used to transfer heat and withstand high electric stress, an increase in flow speeds, and flow electrification problems, particularly in high-voltage forced-oil-cooled power transformers (6). In these transformers, insulating oils are used for both electrical insulation and heat transfer, with the oil circulated from the windings of the transformer to heat exchangers so that the transformer can be operated at higher power levels. With paper cellulose pressboard providing an insulating support structure for the windings and the oil itself being insulating, there are numerous locations for charge accumulation to occur.

The predominant charge separation process in electric power transformers occurs in the insulation ducts composed of insulation paper wrapped coils and pressboard washers, as illustrated in Fig. 3. Typically positive charge on the liquid side of the paper/liquid interface is entrained by the flowing liquid and relaxes downstream onto insulated interfaces or to ground while negative charge on the paper leaks to ground through the coil windings, iron core, and tank walls. Most electrical discharges occur at the bottom of the windings as a surface discharge along the pressboard washers or in the header space above the windings as a volume discharge through the transformer oil (7,8). Surface tracking along the washers has been observed and heard in unenergized transformers, indicating that at least some of the discharge activity is not associated with the applied voltage. These discharges usually reduce the insulation strength and lead to a major fault when the transformer is energized.

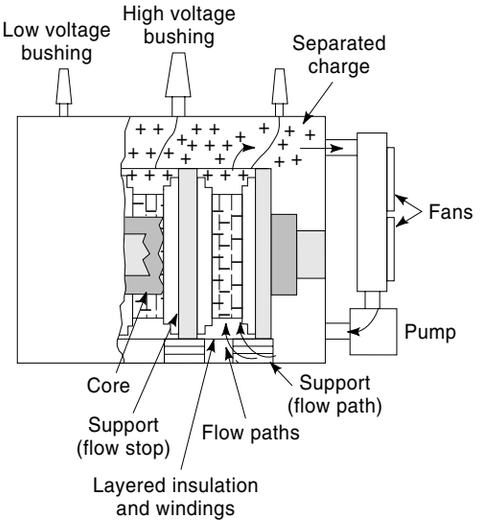

Figure 3. Insulating oil circulated through electric power transformers improves the heat transfer from the windings but also separates the positive and negative charge carriers.

Several of the critical factors which affect the electrification in transformers are the recirculation flow rate, energization, the temperature, and the moisture content. Increasing the flow rate increases the charge separation via the wall shear stress, the charge transport, and the rate of charge accumulation. The application of high voltages and electric fields can enhance charge injection and the charge separation processes at the solid/liquid interfaces. Maximum charging occurs within an intermediate temperature range of 30 to 60 °C due to the temperature dependence of the paper and oil conductivities, the oil viscosity, the moisture partitioning between the paper and oil insulation, and the charge separation at the paper/oil interface (7,9). Water is a ubiquitous impurity and affects the accumulation and leakage processes through the moisture-dependent dielectric losses of the paper insulation.

One scenario for the electrification problem involves the start-up transient when a transformer is being brought into service. As the transformer temperature increases, moisture is driven out of the pressboard insulation into the oil. This moisture initially comes from near the pressboard interface, leaving a relatively dry and highly insulating interfacial zone. Without any leakage, the charge can accumulate on the surface until tracking discharges occur. These discharges cause gas formation which can rise into the high electric field region causing a high-energy discharge and transformer failure. If the failure does not occur during the initial transient, then moisture deep in the pressboard has time to diffuse to the surface. This moisture increases the leakage through the interfacial dry zone so that the surface charge density cannot

give rise to electric field strengths beyond the breakdown strength of oil and pressboard.

The solutions developed for fuels are not always applicable to electric power equipment. For example, grounded conductors are not possible in high field regions and raising the conductivity of the insulating fluid with anti-static additives increases the electrical losses which makes the device less efficient. The main technique for reducing the electrification hazard is to lower the coolant flow rate, even though this can limit the power rating of the equipment. New transformers are designed to operate with lower oil flow rates while existing units use automatic pump controls so that the pumps are only activated when the unit is at an elevated temperature. Nonionizable anti-static additives, such as 1,2,3-benzotriazole, appear to reduce the charge separation at the solid/liquid interfaces and act as electrification suppressants with a minimal effect on the liquid conductivity (10).

Automotive Industry

The increased usage of polymeric materials in automobiles has also led to concerns about flow electrification (11). For example, many of the metal components in the fuel transfer system, such as the lines, pumps, tanks, and filter housings, are being replaced with polymeric components which are light weight and easy to manufacture and install. These polymers tend to be electrically insulating so that charge can accumulate and the potential can rise high enough for spark discharges to occur. Even though gasoline is doped with additives to raise its conductivity, the leakage of charge through the liquid is insufficient for preventing the accumulation of charge. This was not a significant problem when metal components were used throughout the fuel system because all of the components were grounded. However, when part of the system can float in potential, such as a metal filter connected by polymeric fuel lines, the electric potential of the filter and the potential distribution along the insulating lines can rise. While the spark discharges are usually to an external ground, repeated discharges at the same location can lead to a *pinhole* leakage of fuel. The fuel can then leak onto a hot surface or create a combustible vapor so that subsequent discharges can ignite the fuel.

Similar to the petroleum industry, the main technique for eliminating the hazard involves increasing the electrical conductivity of the polymeric materials. This serves to effectively ground all of the components in the system, preventing the accumulation of charge and large potential differences. These conductivity enhancing additives are used in combination with other additives for the polymers which help create the desired mechanical properties such as toughness, stress resistance, chemical inertness, and resistance to swelling.

Electronics Industry

Static electrification in the manufacture and handling of silicon wafers can lead to failures in semiconductor devices (12). The static charge is generated by triboelectric effects, where the wafer and another solid are in contact and then separated, and by the flow of filtered air across the wafer. The charge leads to device failure by attracting particles from the air or personnel garments that contaminate the wafer surface or by electrostatic discharges through the dielectric layers. The problem is compounded by the use of electrically insulating wafer carriers that are chosen for their chemical inertness, so that the charge does not leak away from the wafers. Static prevention techniques include ionization sources that neutralize charge in the air flowing across the wafers, conductive (antistatic) garments and discharge wrist straps for the personnel, grounded floor mats, and grounding work station surfaces. Charge neutralizing antistatic coatings can be applied to surfaces except that they also serve as another source of wafer contamination. Electrification also occurs with the aerosol cans of refrigerant often used by electronic technicians when troubleshooting thermally overloaded circuits (13). By successively freezing circuit board components, if the circuit begins to function properly then the thermal problem can be isolated. However, as the refrigerant leaves the can and passes through an insulating polymeric straw it undergoes flow electrification and deposits positive charge onto the circuit board. This causes problems in erasable programmable ROMS and in static RAMS. Charge buildup on the case also induces charge on the active circuit and can lead to breakdown in the device or across air gaps. The simplest way to avoid static buildup is to cover the chip with a thin piece of metal when spraying so that the chip is cooled by contact with the shielding metal but no charge reaches the chip itself. Some coolant manufacturers add a small amount of conducting fluid to the refrigerant to increase the charge relaxation, but even a small amount of conductor deposited on a circuit board can disrupt the proper operation of the circuit.

STAGES AND FACTORS

A detailed description of the individual electrification stages requires combining the chemical kinetics of the ionizable species with the fluid mechanics of the flowing liquid and the electromagnetics associated with the electrical charge. Although this coupling can be complex, separating the electrification processes into the stages of generation, transport, accumulation, and leakage helps elucidate the roles of the various factors.

Charge Generation

Positive and negative ions are created in insulating liquids by the normal dissociation or ionization of trace impurities and additives. This dissociation process can be described in terms of a chemical reaction. Generally, when using additives, the composition of the additive is known so that the exact chemical reaction is specified. When the conduction through the liquid is dominated by trace impurities the composition is unknown and the chemical reaction must be postulated. A simple model for the chemical reaction is to assume that the reacting species obeys the ionic equation

$$\gamma C \underset{k_r}{\overset{k_d}{\rightleftharpoons}} A^{+q} + B^{-q} \tag{1}$$

where C dissociates into a positive ion A and a negative ion B, k_d is the dissociation rate constant, k_r is the recombination rate constant, and q is the magnitude of the ionic charge. The empirical factor γ represents the molecularity of the reaction; it equals half the slope of the logarithm of the conductivity plotted against the logarithm of the concentration of the neutral species C. The ions try to neutralize each other and re-

combine in the bulk of the liquid, but at boundaries there is a preferential adsorption of one species with the opposite carrier diffusely distributed over a thin boundary region called the electrical double layer. The degree of net charge and the depth to which it penetrates into the liquid volume are related by the balance of ion diffusion, migration, and convection. In stationary equilibrium, diffusion due to concentration gradients is balanced by the electric field induced by the separated charges. This is similar to the distribution of electrons and holes in a semiconductor p–n junction.

As a result of the chemical reactions, the concentrations of the individual species will change with both time and spatial position. By balancing the time rate of change of the concentration of each species in a differential volume with the chemical reactions and the flux through the surface enclosing the volume, the conservation equation for the positive and negative ions becomes

$$\frac{\partial n_\pm}{\partial t} + \nabla \cdot \vec{\mathbf{\Gamma}}_\pm = k_\mathrm{d} n_\mathrm{c}^\gamma - k_\mathrm{r} n_+ n_- \tag{2}$$

where $n_\pm$ is the concentration and $\vec{\mathbf{\Gamma}}_\pm$ is the flux per unit area of the positive and negative species (equivalent to the current density per unit charge) and n_c is the concentration of the neutral species. The first term on the right side gives the generation rate of the ions while the second term gives the rate of recombination of the ions to form the neutral molecule. The flux term gives the transport of each species through the fluid and generally contains contributions due to diffusion, convection, and drift. The constitutive law for the flux per unit area is

$$\vec{\mathbf{\Gamma}}_\pm = -D_\pm \nabla n_\pm + n_\pm \vec{\boldsymbol{v}} \pm \mu_\pm n_\pm \vec{\boldsymbol{E}} \tag{3}$$

where $D_\pm$ is the diffusivity, $\vec{\boldsymbol{v}}$ is the fluid velocity, $\mu_\pm$ is the ion mobility, and $\vec{\boldsymbol{E}}$ is the electric field. Einstein's relation relates the diffusivity and mobility to the thermal voltage

$$\frac{D_\pm}{\mu_\pm} = \frac{kT}{q} \tag{4}$$

where $k = 1.38 \times 10^{-23}$ J/K is Boltzmann's constant and T is the absolute temperature. The electric field is related to the potential distribution Φ by $\vec{\boldsymbol{E}} = -\nabla\Phi$.

In stationary equilibrium $\vec{\boldsymbol{v}} = 0$ and the flux of each ion is zero, $\vec{\mathbf{\Gamma}}_\pm = 0$, so that Eqs. (3) and (4) require that the ion concentrations obey Boltzmann distributions as

$$n_\pm(x) = n_\mathrm{o} \mathrm{e}^{\mp q\Phi(x)/kT} \tag{5}$$

where n_o is the equilibrium concentration of each ion when the potential is zero. With the net charge density defined by $\rho \equiv q(n_+ - n_-)$ and a dielectric permittivity of ϵ, Eq. (5) in Poisson's equation yields

$$\nabla^2\Phi = -\frac{q}{\epsilon}(n_+ - n_-) = \frac{2qn_\mathrm{o}}{\epsilon} \sinh\frac{q\Phi}{kT} \tag{6}$$

which is the Poisson–Boltzmann equation. Generally, this equation must be solved with the conservation equations for both carriers [Eq. (2)] and the neutral species, including the finite recombination and dissociation rates. However, in situations where the local concentrations of each carrier are not far from their equilibrium values, a good approximation is that the potentials are much less than the thermal voltage, $q\Phi/kT \ll 1$. Then, Eq. (6) can be linearized to

$$\nabla^2\Phi - \frac{\Phi}{\lambda^2} = 0 \tag{7}$$

where

$$\lambda = \sqrt{\frac{\epsilon kT}{2q^2 n_0}} = \sqrt{\frac{\epsilon D_\pm}{2qn_0\mu_\pm}} \approx \sqrt{\frac{\epsilon D}{\sigma}} \tag{8}$$

is the Debye length and indicates the length scale of noncharge neutrality near the interface. The last equality in Eq. (8) relates the Debye length to the ohmic conductivity $\sigma = qn_0(\mu_+ + \mu_-) \approx 2qn_0\mu_\pm$ assuming $\mu_+ \approx \mu_-$ so that $D_+ \approx D_- = D$. To simulate the preferential adsorption of charge onto a solid/liquid interface, assume that the interface can be modeled as a charged sheet with potential ζ at $x = 0$. On the liquid side of the interface ($x > 0$), the potential, electric field, and the charge density obey

$$\begin{aligned} \Phi &= \zeta e^{-x/\lambda} \\ E_\mathrm{x} &= -\frac{d\Phi}{dx} = \frac{\zeta}{\lambda} e^{-x/\lambda} \\ \rho &= \epsilon \frac{dE_\mathrm{x}}{dx} = -\frac{\epsilon\zeta}{\lambda^2} e^{-x/\lambda} \end{aligned} \tag{9}$$

The volume charge density on the liquid side of the interface, called the *wall* charge density ρ_w, is related to the zeta potential as $\rho_\mathrm{w} = \rho(x = 0) = -\epsilon\zeta/\lambda^2$. It follows from Eq. (5) that the wall concentrations of the ionic species are also related to the zeta potential by $n_\pm(x = 0) = n_0(1 \mp q\zeta/kT)$. Often the zeta potential and the Debye length are used to characterize the interface since the carrier concentration, charge density, and field distribution can be calculated from them.

Depending on the properties of the electrolytic solution, the potential and charge distributions of Eq. (9) can be maintained in the presence of an externally applied electric field and fluid convection. Consider an aqueous solution at room temperature where $\sigma \sim 0.1$ S/m, $D \sim 10^{-10}$ m^2/s, and $\epsilon \approx 80\epsilon_0 \approx 700$ pF/m so that $\lambda \approx 0.8$ nm, which is quite small. A zeta potential of order of the thermal voltage at room temperature ($\zeta \approx 25$ mV) across this double layer yields a large internal electric field of $E_\mathrm{x} \approx \zeta/\lambda \approx 30$ MV/m. Because of the large electrical conductivity in these solutions, externally applied fields cannot approach such magnitudes and thus hardly disturb the equilibrium of the double layer. Similarly, convection has a negligible effect on the double layer as seen by comparing the electrical relaxation time $\tau_\mathrm{e} = \epsilon/\sigma \approx 7$ ns to a liquid transport time $\tau_\mathrm{l} = L/U$ where L is a characteristic travel length for a fluid moving with velocity U. For a representative length of $L = 1$ cm and velocity $U = 1$ m/s, $\tau_\mathrm{l} = 0.01$ s is much greater than τ_e, indicating that the charge in the fluid can redistribute rapidly compared to the imposed fluid convection. The ratio of the dielectric relaxation time to the transport time is the electric Reynold's number $R_\mathrm{e} = \tau_\mathrm{e}/\tau_\mathrm{l} = \epsilon U/\sigma L \approx 10^{-6}$. Because $R_\mathrm{e} \ll 1$, convection in aqueous electrolytes usually does not disturb the charge distribution in the double layer.

In contrast, external electric fields and imposed fluid convection can greatly alter the charge distribution in the double layer for highly insulating nonaqueous fluids. As an example, consider transformer oil which has room temperature properties of $\sigma \sim 1$ pS/m, $\epsilon \approx 2.2\epsilon_0 \approx 19.5$ pF/m and viscosity $\eta \approx 0.02$ N-s/m^2. The mobility of the ions in hydrocarbon liquids is empirically related to the viscosity by Walden's rule

$$\mu \approx \frac{2 \times 10^{-11}}{\eta} [\text{m}^2/(\text{V-s})] \tag{10}$$

For transformer oil this yields $\mu \approx 10^{-9}$ m^2/(V-s) and a molecular diffusion coefficient from Eq. (4) of $D \approx 2.5 \times 10^{-11}$ m^2/s. The corresponding Debye length is $\lambda \approx 22$ μm and the internal electric field is then $E_x \approx 1.1$ kV/m. With such low internal electric fields, reasonable externally applied fields are significant in determining the charge distribution in the double layer. With a relaxation time of $\tau_e \approx 20$ s, the electric Reynold's number $R_e \approx 2000$ is large and fluid convection also strongly influences the distribution of charge in the double layer.

Charge Transport

Electrification occurs when the mobile portion of the electrical double is entrained in the fluid flow. In general the fluid velocity also depends on the electrical forces on the charged species, as in electrophoresis and electroosmosis, even when the charged species are present in trace amounts. However, usually when flow electrification is a problem the fluid velocity is primarily imposed by an external system such as a pump and the electrical forces on the particles can be neglected. The fluid flow is governed by the Navier–Stokes equation

$$\rho_m \frac{D\vec{v}}{Dt} = -\nabla p + \eta \nabla^2 \vec{v} + \vec{F}_e \tag{11}$$

where ρ_m is the mass density, $D/Dt \equiv \partial/\partial t + \vec{v} \cdot \nabla$ denotes the convective derivative, p is the pressure, and $\vec{F}_e$ denotes external forces applied to the system, such as gravity. For low-viscosity liquids the velocity of the liquid is determined by the fluid viscosity. As the mean velocity U increases, the inertial effects become important. The nondimensional parameter that describes the relative importance of the inertial and the viscous effects on the flow is the hydrodynamic Reynold's number $R = \rho_m UL/\eta$ where L is a characteristic system length. For small Reynold's numbers the flow is smooth and steady (laminar) while at moderate and large Reynold's numbers the flow becomes agitated with rapid fluctuations (turbulent).

To illustrate the role of the fluid velocity, the streaming current through conducting pipes will be calculated for both laminar and turbulent flows. The pipe flow model is important because the transport of liquids through pipes was an initial problem in the petroleum industry and it resembles other structures such as the pores in filter paper and the flow ducts in an electric power transformer. It serves as a model system for both experimental and theoretical investigations.

Laminar Flow. The flow is in the laminar regime when the hydrodynamic Reynold's number is low. With the flow velocity zero at the wall, the fully developed flow velocity distribution in a pipe of radius a and average velocity U is

$$v_z(r) = 2U\left[1 - \left(\frac{r}{a}\right)^2\right] \tag{12}$$

The corresponding streaming current I is

$$I = \int_0^a \rho(r) v_z(r) 2\pi r \, dr \tag{13}$$

For typical pipe dimensions the Debye length λ is much smaller than the radius of the pipe, and the small fluid velocity within the double layer has little effect on the charge distribution. Defining $x = a - r$ as the distance from the pipe wall, the charge distribution is approximately given by Eq. (9) and the velocity near the pipe wall is approximately $v_z \approx 4Ux/a$. Substitution into Eq. (13) gives the approximate streaming current as

$$I \approx \int_0^\infty \rho(x) 8U\pi x \, dx = 8\pi U \rho_w \lambda^2 \tag{14}$$

Thus, for laminar flow the streaming current increases linearly with the flow rate and is proportional to the wall charge density or the zeta potential. Modifications to this expression are required when the fluid flow or charge distribution development lengths are long compared to the length of the tube (see Eq. 17) or when the radius of the tube is comparable to the Debye length (14,15).

Turbulent Flow. The flow is in the turbulent regime when the hydrodynamic Reynold's number is large. As the flow velocity is increased, in addition to a mean flow the flow profile has rapidly varying fluctuations in time and space. These velocities fluctuate about a mean value with variations generally large compared to the mean value. The fluid paths are extremely complicated and result in extensive mixing which greatly alters the charge distribution and the amount of convected charge. This enhanced mixing is sometimes expressed in terms of a turbulence enhanced effective molecular diffusivity D_T. The turbulent mixing leads to a core region where the carrier concentrations are essentially uniform (if the Debye length based on D_T is much greater than the pipe radius). At the edge of this region, near the boundaries diffusion sublayers develop in which molecular diffusion and drift dominate the convective mixing of the turbulent flow. The thickness of the sublayer δ is usually taken as the distance where the molecular and turbulent diffusivities are equal.

For pipe flow, Abedian and Sonin derived an expression for the convection current carried in a pipe of radius a (16). For a fluid with an average velocity U and kinematic viscosity $\nu = \eta/\rho_m$, empirical correlations give a pipe wall shear stress τ_w of

$$\tau_w \approx 0.0396 \rho_m U^2 R^{-1/4} \qquad 4000 < R < 100,000$$

(Blasius correlation) (15)

and a sublayer thickness of

$$\delta \approx \frac{11.7\nu}{(\nu/D)^{1/3}(\tau_w/\rho_m)^{1/2}} \approx 117.6 R^{-7/8} \frac{a}{(\nu/D)^{1/3}} \tag{16}$$

where the hydrodynamic Reynold's number is $R = 2Ua/\nu$. The steady-state streaming current can be expressed as

$$I = I_\infty \left(1 - e^{-z/L_e}\right) + I_0(z = 0)e^{-z/L_e} \tag{17}$$

where z is the axial distance along the length of the pipe, I_0 is the initial streaming current at the $z = 0$ entrance to the pipe section, and I_∞ is the streaming current for a pipe with length much longer than the development length L_e, defined in terms of the wall charge density ρ_w by

$$\frac{I_\infty}{\rho_w \pi a^2 U} = \frac{R\tau_w \lambda^2}{\rho_m U^2 a^2}\left[1 - \frac{\delta/\lambda}{\sinh \delta/\lambda}\right] + \frac{\delta/\lambda}{\sinh \delta/\lambda}\frac{1}{1 + a\delta/2\lambda^2} \tag{18}$$

$$L_e = \frac{\epsilon U/\sigma}{1 + 2\lambda^2/a\delta} \tag{19}$$

Note that for $\delta \gg \lambda$ the streaming current reduces to the laminar flow streaming current of Eq. (14). In the absence of an inlet current, the streaming current, which generally has a larger magnitude than the laminar flow streaming current, is again proportional to the wall charge density but the flow-rate dependence is more complicated. Using this expression, Abedian and Sonin successfully fit a large database of reported streaming currents in hydrocarbon liquids flowing through smooth-walled conducting pipes to a single value of the zeta potential, $\zeta \approx 0.5kT/q \approx 13$ mV (17). Alternative models for pipe flow streaming currents attempt to capture more of the physics of the turbulent mixing and/or the interfacial charge boundary conditions but are generally more complicated and require numerical solutions (18–21).

As described in the previous section, application of an electric field can influence the charge being transported by the liquid, particularly under turbulent flow conditions. For high-voltage ac energization, the maximum displacement for charge carriers of mobility μ by an electric field of amplitude E_0 and radian frequency ω is $2\mu E_0/\omega$. When the electric field direction reverses, the charge returns to the boundary unless the charge has already crossed the diffusion sublayer where it is then entrained in the flow. The critical condition for the turbulent core charge density to be enhanced by the ac electric field is $\delta = 2\mu E_0/\omega$; the maximum displacement of the charge carriers must be greater than the sublayer thickness for the charge to be entrained in the turbulent core region. For dc energization, the dc field enhances the migration of charge across the diffusion sublayers which can lead to an increase in the net charge density in the well-mixed core region of the flow. These fields also cause a net charge to develop on the interfaces in the system, similar to the separation and accumulation of charge inherent in the flow electrification process.

Charge Accumulation

The charge entrained by the liquid flow can accumulate in the volume of the liquid, on insulating surfaces, or isolated conductors. When all of the enclosure surfaces are conducting and grounded, the electric fields due to the separated charge are much smaller than that required for electrical discharges. The fields can only build up to breakdown strength values if there is an isolated conductor or insulating surface which allows surface charge to accumulate at a rate that exceeds the leakage rate. As an example consider an isolating conducting sphere of radius R_s in a dielectric of permittivity ϵ and conductivity σ. The sphere has a capacitance with respect to infinity of $C = 4\pi\epsilon R_s$, which is approximately 2.5 pF for a 1-cm radius sphere in transformer oil ($\epsilon/\epsilon_0 = 2.2$), and a leakage resistance of $R_L = 1/(4\pi\sigma R_s)$ plus any other series leakage resistance through insulating supports to ground. For a constant charging streaming current I the voltage transient for an initially uncharged sphere is

$$v(t) = IR_L\left(1 - e^{-t/R_L C}\right) \tag{20}$$

At short times ($t \ll R_L C$) the voltage increases linearly with time as $V = It/C$. For a streaming current of 2.5 nA, the voltage increases at a rate of 1 kV/s. If the sphere is connected to ground via a leakage resistance R_L the steady-state voltage, if breakdown does not occur first, is $V_s = IR_L$. With a streaming current of 2.5 nA, this voltage can exceed 100 kV if R_L exceeds 40 TΩ. If R_L is only limited by the leakage through the oil then the time constant $R_L C$ for the potential rise equals the dielectric relaxation time $\tau_e = \epsilon/\sigma$. To limit the steady-state voltage rise to less than 100 kV, $\tau_e = R_L C$ must be less than 100 s.

Insulating solids and pipes allow charge to accumulate along the solid/liquid interface. If the surface served as the initial source of charge then the net surface charge density increases as the entrained diffuse charge is transported away by the flow. If the surface is at a downstream location from the charge source then charge entrained in the liquid can relax onto the surface. If the insulating pipe is surrounded by a conductor or has a grounded conductor nearby, the field in the insulating pipe wall could become very high, exceeding the breakdown strength of the dielectric to initiate a spark discharge.

Charge Leakage

For insulating surfaces or isolated conductors, charge leakage through surfaces and the volume determines the steady-state potential distribution. This leakage is represented by the term R_L in Eq. (20). If the leakage resistance is too high, the potentials can exceed breakdown values and there is a discharge. To increase the leakage, anti-static additives are often used. Shell ASA-3, a xylene-based solution of chromium and calcium organic salts stabilized with a polymer, is typically used with jet fuels. By weight it is $\frac{1}{2}$ xylene, $\frac{1}{6}$ chromium alkyl salicylate, $\frac{1}{6}$ calcium disulfosuccinate (Aerosol OT), and $\frac{1}{6}$ polymethylmethacrylate dispersant (copolymer of alkyl methacrylate and vinyl pyridine). Hydrocarbon fuels usually have intrinsic conductivities in the range of 0.1 pS/m to 10 pS/m at room temperature. The recommended safe conductivity range is 50 pS/m to 300 pS/m and is achieved by adding approximately 0.5 g/m^3 ASA-3 to the fuel.

The ionizable additive DCA-48 increases the bulk conductivity of the liquid but also affects the solid/liquid interface (22). It is a steric amine salt having a molecular weight of approximately 6000 and contains 24 to 28 diamine-carboxylic functional groups. It has been used as an antistatic additive in trichlorotrifluoroethane (Freon 113 or Freon TF) in a compact high-voltage dc valve where the Freon was circulated through insulating Tefzel (a modified copolymer of ethylene and polytetrafluoroethylene) tubing as a coolant. Adding

DCA-48 raises the liquid conductivity (up to 0.2 pS/m) and reduces the electrification streaming current. Measured relaxation times decrease with time while the bulk liquid conductivity is constant, suggesting that the DCA-48 also increases the interfacial conductivity.

Another technique for increasing the leakage losses is to modify the configuration of the system. If one component of the system, such as the pump or the filter in a fuel line, is acting as a charge source, one may be able to place a relaxation region, such as a grounded expansion volume or conducting pipe, immediately downstream from the source. This helps to limit the charge reaching downstream locations. Another example, currently used in electric power transformers, is to modify the coolant flow pattern so that lower flow rates are necessary for maintaining the temperature of the apparatus.

Factors

Table 1 summarizes many of the factors known to affect electrification stages when a dielectric fluid is pumped across a solid surface. The solid is usually taken to be insulating, but the electrification of metallic solids is also considered. For transformers, the solid is a paper insulation. In other systems, such as fuel transfer and processing systems, it can be a polymeric or metal enclosure. Energization applies primarily to electric power apparatus. These factors contribute to hazardous field buildup through the four electrification stages: charge generation, transport, accumulation, and leakage.

Each of the factors in Table 1 generally affects more than one stage. For example, trace materials either inadvertently present or added to control electrification can contribute to the charging phase by selective ion adsorption at interfaces which causes the initial charge separation. This same material may also increase the conductivity of the fluid to enhance charge relaxation through the volume or over time add to the surface conductivity at the interface increasing leakage, thereby helping to alleviate the electrification problem. A similar dual role is possible with moisture which adds to leakage in the volume and at interfaces, and so thereby also alters the field distribution with and without energization which can affect the field-dependent injected charge density. Grounded metal conductors in the flow, thought to provide a path to ground for impacting charge, may actually provide a surface and thus a source of additional streaming current.

MEASUREMENT TECHNIQUES

Although there are many different diagnostic techniques for characterizing the electrification processes, all of them involve measuring the voltage rise of an isolated structure, the electric field around an isolated structure or the streaming current through a structure. Based on these measurements the charge entrained in the flowing liquid or the accumulated surface charge can be measured. These measurements allow the effects of the various factors in the previous section to be quantified.

Generic Flow Models

Many electrification experiments use a continuous flow model similar to that shown in Figure 4a (22,23). The structure to be tested, such as a conducting or insulating pipe, a filter or a pressboard duct with spacer blocks, is placed between two isolated fittings in a flow line. Pressurized dry nitrogen gas forces the test liquid through the pipes, the test structure,

Table 1. Factors Affecting the Electrification Stages

	Stages			
Factors	Generation	Transport	Accumulation	Leakage
Flow rate; turbulence	Streaming current; diffusion sublayer; turbulent diffusion	Reynold's No.; flow profile; diffusion sublayer thickness; wall shear stress		Residence time
Temperature	Reaction kinetics; Debye length; diffusion sublayer; Arrhenius	Viscosity (Reynold's No.)		Liquid and solid conductivity; moisture equilibrium
Contaminants; additives; surface active agents	Zeta potential; adsorption; charge injection		Selective adsorption	Enhanced conduction
Configuration	Inlet current from upstream sources (pumps, ducts, grounded pipes), liquid/solid interface	Cooling ducts; entrance and exit regions; headers	Upper plenum; liquid/solid interfaces; charge deposition from upstream injection	Liquid, solid, and liquid/solid interfacial conductivity; grounded conducting surfaces
Surface condition	Roughness; turbulence	Wall shear stress		
Energization	Charge injection	Electroconvection		
Electrical charging tendency (ECT)	Charge buildup on duct walls; charge buildup in liquid volume	Entrainment of mobile double layer charge	Entrained charge accumulates on isolated surfaces	
Dielectric strength	Discharges due to potential buildup			Tracking; surface discharges; bulk discharges
Moisture	Source of ions at liquid/solid interface			Liquid, solid, and liquid/solid interfacial conductivity

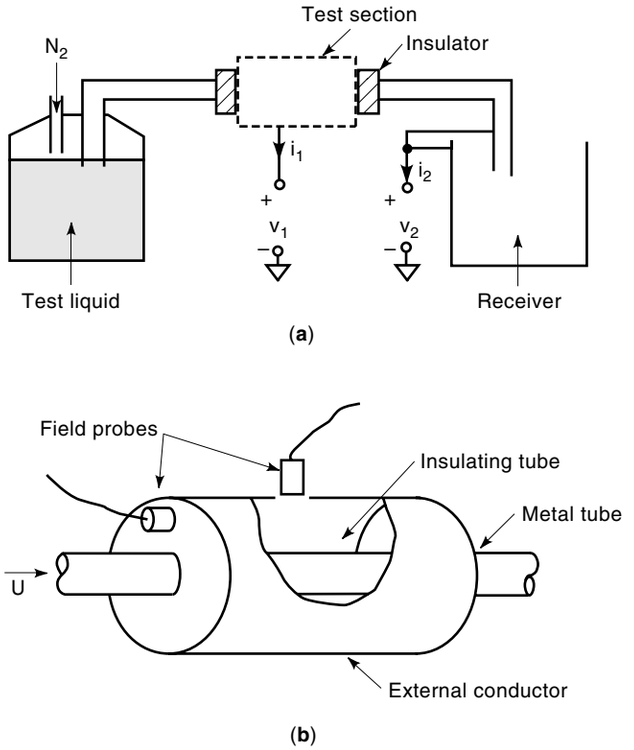

Figure 4. (a) A generic flow model in which the streaming current or voltage of a test structure or a receiving unit is monitored and related to the electrification processes inside the test structure. (b) Electric field components around insulating structures are measured with noncontacting field probes.

and into the receiver. Monitoring the streaming current i_1 from the test structure or i_2 from the receiving vessel and downstream conducting pipes allows the charge density ρ entrained by the flow to be calculated from

$$\rho = \frac{i_1}{Q} = \frac{i_2}{Q} \tag{21}$$

where Q is the volume flow rate. Generally, measurement of the current to an isolated structure gives the difference between the current leaving and the current entering the structure, and any structure simultaneously acts as both a relaxation region for entering charge and as a charging region for internally separated charge. To use Eq. (21) one must ensure that the inlet fluid is uncharged; one way to minimize the inlet current is to place a relaxation volume before the inlet. For insulating structures and pipes, Fig. 4(b) shows that the radial and axial electric field components can be measured by noncontacting field probes in the wall of a grounded surrounding metallic enclosure. The axial electric field component which drives surface leakage can be greatly minimized at the expense of increasing the radial field by making the enclosure a tightly fitting sleeve. Current and potential distributions along insulating pipes can be measured from the leakage current and surface potential of segmented electrodes surrounding the pipe.

For complicated structures, such as filters inside insulating housings, both the streaming potential and noncontacting field probes can be used simultaneously. The streaming current provides a measure of the charge entrained in the flow and carried downstream while the field probe can measure the dynamics of the net charge left behind. For the case of the filter, the charge can leak away from the filter paper onto the insulating housing so that large electric fields can be present both inside and outside the filter housing. As another variation of this measurement technique, the charge generated by flow sources such as pumps can be measured by minimizing the length of the inlet pipe section and running the flow directly into the receiver.

Electrostatic Charging Tendency

The most common laboratory technique for characterizing electrostatic charging tendency (ECT) is the ministatic tester shown in Fig. 5. It was initially developed for jet fuel measurements by Exxon Research and the Naval Research Laboratory (3) but was adapted to transformer oil measurements by Westinghouse (24). The ECT is measured by forcing the liquid of interest through standard filter paper which is a high-grade cellulose material. The same filters are used for transformer oils because the paper insulation in transformers is not sufficiently porous for adequate fluid flow. The current from ground necessary to compensate double layer charge entrained in the fluid is measured, or equivalently the current to the receiver grounded through a low impedance electrometer is measured. The numerous pores in the filter increases the effective area and thereby increases the streaming current. At volumetric flow rates of $Q = 1$ cm^3/s to 2 cm^3/s, charging currents i are typically in the range of 10 pA to 1 nA. From Eq. (21), the associated charge density ranges from 5 μC/m^3 to 1000 μC/m^3, with low charging liquids usually having charge densities below 25 μC/m^3. This approach is fast and simple for comparing the relative charging tendencies of different liquid samples against a particular material filter. Changing the type of filter generally changes the charging

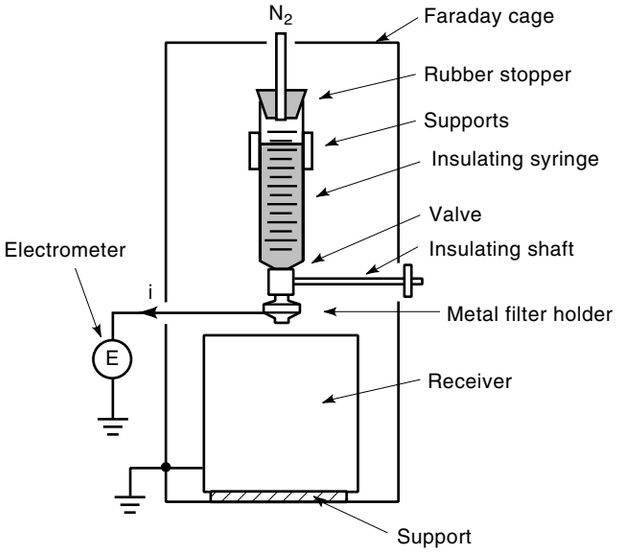

Figure 5. The electrostatic charging tendency of a liquid is measured in the Ministatic tester by measuring the current created by pressurized flow through a filter.

level but usually does not change the ranking levels of different liquids.

Charge Density Measurements

Although terminal voltage and current measurements on a structure provide useful information about the electrification process, a direct measure of the charge entrained by the flow is also possible.

Conducting Probes. Early attempts at directly measuring the charge density of the fluid involved placing conducting probes into the flowing liquid and measuring the open circuit voltage or short circuit current. One example is a charge density probe composed of three equally spaced parallel circular plates (9). The outer two electrodes are grounded and the charging potential V_p of the center electrode is measured by a high-impedance electrometer. Assuming that the charge density ρ is uniform, integrating Gauss' law across the dielectric and solving for the charging potential yields

$$V_p = \frac{\rho d^2}{2\epsilon} \tag{22}$$

where d is the separation distance between the plates. Unfortunately, this does not provide an unambiguous value for the charge density since one may never be certain to the extent to which the probe response is due to impacting charge from the flow or from charge that is removed from the probe by the same charge separation process that is being studied. Fluid flowing through the probe, even if entering uncharged, will separate some charge from the electrode surfaces, raising the measured potential. There is no way to separate the effects of entering charge due to upstream flow electrification from charge separation within the probe.

Absolute Charge Sensor. The absolute charge sensor (ACS) shown in Fig. 6 measures the charge density independent of the fluid's electrical properties, the velocity of the fluid, and any electrification process within the instrument (25). A sample of the fluid is pumped into a Faraday cage by an expandable metal bellows driven by a linear actuator. The electrically isolated Faraday cage is connected to ground by an electrometer so that the measured short-circuit current or open-circuit voltage is directly proportional to the fluid charge density. The probe entrance is shielded so that streaming currents generated from electrification on the outer surface of the probe are not measured. The three-way valve allows the sampled fluid to be returned to the system at a downstream location or a relaxation region so that the exiting fluid is not in the proximity of the sampling probe.

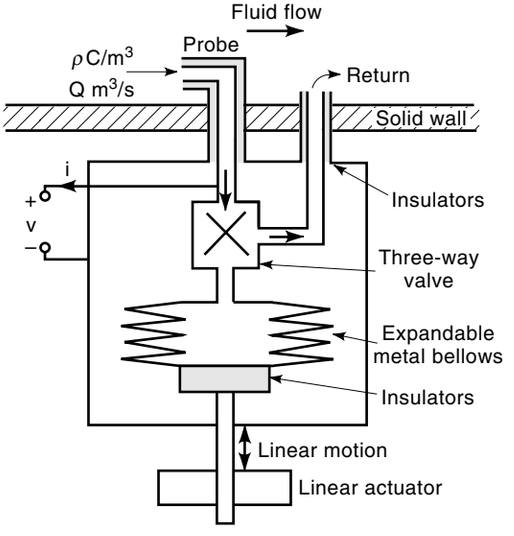

Figure 6. The absolute charge sensor (ACS) measures the net charge density entrained in the flow by sampling a portion of the fluid.

The charge density is calculated from the known filling flow rate and the measured current or voltage, depending on the measurement mode of the electrometer. A charged body introduced into a Faraday cage induces an opposite polarity charge on the interior wall of the conducting volume. Thus, without actually being transported to the wall, the net charge induced onto the conductive inner wall would be equal to but of opposite polarity to that in the fluid. Because the rate of accumulation of the charge so induced in the inner wall of the container comprises a capacitive electrical current that can be measured externally, it is possible to measure this net charge with an electrometer. In addition to the image charge, there is a conduction current associated with the relaxation of the charged fluid and a current due to flow-induced electrification on the internal surfaces of the ACS volume. However, because the total charge within the Faraday cage volume whether due to imaging, charge relaxation, or electrification remains constant, with no fluid leaving the Faraday cage during the measurement, the measured current i depends only on the inlet convection current. For inlet flow rate Q, the fluid charge density is calculated from Eq. (21). Except for possible electrification effects at the tip of the sampling probe, this device provides an absolute measure of the charge density.

Tandem Charge Monitor. An alternative to the ACS that does not require moving parts is the tandem charge monitor (TCM) (26). The TCM consists of two identical shielded chambers through which the dielectric fluid passes with laminar flow. Each chamber is virtually grounded through electrometers which measure the currents i_1 in the upstream chamber and i_2 in the downstream chamber. These currents reflect the fluid residence time and dielectric relaxation time in each chamber. The charge density in the entering fluid is then computed from

$$\rho = \frac{i_1}{(1 - i_2/i_1)Q} \tag{23}$$

where Q is the volume flow rate of the fluid. This expression is independent of the fluid conductivity and is valid even if the fluid still contains charge as it exits the second chamber. The flow through the device is maintained by either the pressure drop between the sampling and return ports or by an external pump on the return line.

Rotating Electrode Measurements

Rotating disk and cylinder electrode apparatuses are commonly used to investigate interfacial chemical kinetics. In these apparatuses, measurements of the current or voltage of

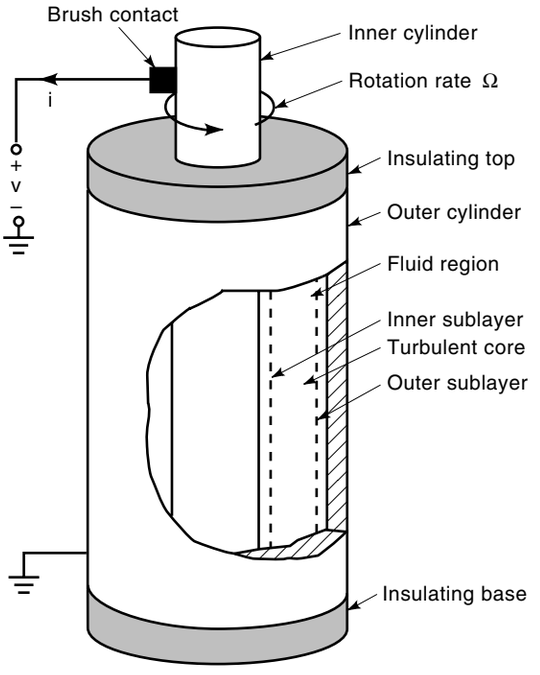

Figure 7. In a rotating cylinder apparatus, rotation of the inner cylinder generates fluid flow and separates charge. Measurements of the terminal voltage, terminal current, and charge density in the turbulent core region characterize the electrification processes.

the disk or electrode via a brush contact are correlated to the interfacial transport properties (1). The rotating cylinder electrode apparatus shown in Fig. 7 has been used extensively to investigate electrification effects for many semi-insulating liquid/solid combinations because it offers many advantages over pipe flow measurements (27,28). The fluid under test fills the annulus between cylinders that are covered with the solid material to be tested such as oil-impregnated paper backed by metal. The rotation rate of the inner cylinder is varied to give controlled laminar or turbulent flows. This compact apparatus allows for flexibility in testing liquids, trace impurities, and solid insulation without involving large amounts of material and allows the materials to be easily changed. By virtue of the re-entrant flow, it acts like a pipe of infinite length and thus provides for the measurement of basic electrification parameters even in highly insulating systems, where the electrical development length L_e in Eq. (19) for a pipe flow system is likely to be longer than the practical length of a test section. By sampling the charge entrained in the azimuthal flow at a sufficiently slow rate to not disturb the azimuthal flow, equilibrium electrification parameters can be deduced. The flow Reynolds number, and thus the diffusion sublayer thicknesses analogous to that given in Eq. (16), is set by the shaft rotational velocity of the inner cylinder, independent of the flow rate used to sample the charge carried by the liquid. Effects of energization can also be studied with the brush contact allowing a high voltage to be imposed. The brush contacts also allow measurement of open-circuit terminal voltage and short-circuit current due to inner cylinder rotation which can be related to the volume charge density. To measure the charge entrained in the fluid flow, the rotating cylindrical electrode apparatus can be used as the test structure of Fig. 4 or the ACS or TCM probes can be inserted through the stationary outer wall into the turbulent fluid core.

Similar to the streaming current calculation in turbulent pipe flow, the terminal measurements and the core charge density are related to the rotation rate of the inner cylindrical electrode (29). Empirical studies give the sublayer thickness δ_i at the inner cylinder and δ_o at the outer cylinder as

$$\frac{\delta_i}{R_i} = \frac{\delta_o}{R_o} \approx \frac{3.3}{Sc^{0.356} R C_f} \tag{24}$$

where R_i is the inner cylinder radius, R_o is the outer cylinder radius in contact with the fluid, $R \equiv 2\Omega R_i^2/\nu$ is the Reynolds number, Ω is the inner cylinder angular velocity, $Sc \equiv \nu/D$ is the Schmidt number, and C_f is the drag coefficient given by

$$\frac{1}{\sqrt{C_f}} \approx -0.6 - 4.07 \log_{10}\left(\frac{2}{R\sqrt{C_f}}\right); \quad 8 \times 10^2 < R < 8 \times 10^5 \tag{25}$$

For bare metal electrodes the turbulent core volume charge density under open circuit conditions is

$$\rho_o = \frac{2\lambda}{R_o\left[1 - \left(\frac{R_i}{R_o}\right)^2\right]}\left[\frac{\rho_{w,o}}{\sinh\left(\frac{\delta_o}{\lambda}\right)} + \frac{R_i}{R_o}\frac{\rho_{w,i}}{\sinh\left(\frac{\delta_i}{\lambda}\right)}\right] \tag{26}$$

with open-circuit voltage

$$v_o = \frac{\lambda}{\epsilon}\left\{\frac{R_o \rho_{w,o}}{\sinh\left(\frac{\delta_o}{\lambda}\right)}\left[\frac{1}{2} + \left(\frac{R_i}{R_o}\right)^2 \frac{\ln\left(\frac{R_i}{R_o}\right)}{1 - \left(\frac{R_i}{R_o}\right)^2}\right] + \frac{R_i \rho_{w,i}}{\sinh\left(\frac{\delta_i}{\lambda}\right)}\left[\frac{1}{2} + \frac{\ln\left(\frac{R_i}{R_o}\right)}{1 - \left(\frac{R_i}{R_o}\right)^2}\right]\right\} \tag{27}$$

The short-circuit current is

$$i_s = \frac{2\pi H \sigma v_o}{\ln\left(\frac{R_o}{R_i}\right) + \frac{D}{\lambda}\left\{\frac{1}{k_o \sinh\left(\frac{\delta_o}{\lambda}\right)}\left[\frac{1}{2} + \left(\frac{R_i}{R_o}\right)^2 \frac{\ln\left(\frac{R_i}{R_o}\right)}{1 - \left(\frac{R_i}{R_o}\right)^2}\right] + \frac{1}{k_i \sinh\left(\frac{\delta_i}{\lambda}\right)}\left[\frac{1}{2} + \frac{\ln\left(\frac{R_i}{R_o}\right)}{1 - \left(\frac{R_i}{R_o}\right)^2}\right]\right\}} \tag{28}$$

and the short-circuit turbulent core volume charge density is

$$\rho_s = \rho_o + \frac{\lambda}{\pi H\left(R_o^2 - R_i^2\right)}\left[\frac{1}{k_i \sinh\left(\frac{\delta_i}{\lambda}\right)} - \frac{1}{k_o \sinh\left(\frac{\delta_o}{\lambda}\right)}\right] i_s \tag{29}$$

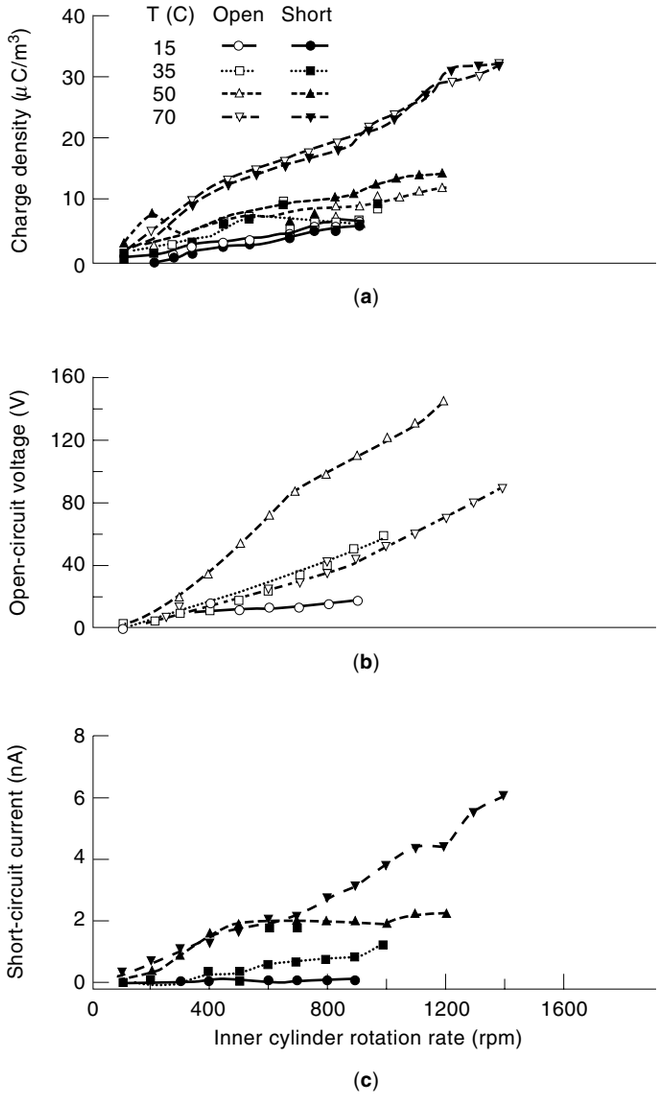

Figure 8. Increasing the rotation rate of the inner cylinder increases the core charge density (a), the open-circuit voltage (b), and the short-circuit current (c). The charge density and current also increase with temperature but the voltage reaches a maximum at intermediate temperatures.

where H is the height of the cylinders, and k_i and k_o are surface reaction velocities at the inner and outer cylinder interfaces. This shows that the charge density in the core region depends on the current flowing through the interface. The reaction velocities are only involved when there is a net current flow across the interface. The core charge density, voltage, and current become larger as the rotation rate increases and the sublayer thickness becomes small compared to the Debye length. Figure 8 shows a representative set of data for transformer oil filling the gap between stainless steel cylinders as a function of the inner cylinder rotation rate.

FUTURE CONSIDERATIONS

Although many of the basic electrification processes associated with the separation and accumulation of charge are well understood, one important phenomenon is still unresolved: the interfacial charge-transfer process (30). This is not surprising since the ions responsible for the charge separation at the electrical double layer typically come from the ionization of uncontrolled trace impurities. This limits the effectiveness with which one can isolate the effects of the various factors, such as the additive 1,2,3-benzotriazole (BTA), on the interfacial charge transport. Several boundary conditions have been postulated to represent this charge transfer, including a constant wall charge density (k_i, $k_o \to \infty$) in Eqs. (28) and (29), a constant interfacial zeta potential (17), or spatial derivative of the charge density at the walls (31). Although these models provide a reasonable representation of the equilibrium interfacial boundary condition, it is not obvious that these equilibrium results can simply be extended to the nonequilibrium case.

Current research in the field is focussing on understanding the interfacial kinetics and coupling the effects of finite charge transfer reaction rates and accumulated surface charge on the charge entrained in the electrical double layer (18,29,32). An example pertaining to power transformers is the controversy surrounding the benefits of the additive BTA. Japanese transformer manufacturers add approximately 5 to 50 μg/g BTA to the oil to reduce the electrification, but measurements show that the BTA concentration decreases with time and the magnitude of the electrification streaming current does not always decrease with addition of BTA (10). Fortunately, the compact rotating cylindrical electrode apparatus of Fig. 7 is well-suited to this type of investigation. By using core charge density, open-circuit voltage and short-circuit current measurements similar to Fig. 8, the effect of BTA on the interfacial wall charge densities can be estimated, as shown in Fig. 9 for a pressboard/transformer oil interface (29). Although this shows the surface-modifying behavior of the BTA as the wall charge density decreases for oil BTA concentrations greater than approximately 10 μg/g, the nonionizing BTA also reduced the oil conductivity, which increased the Debye length and led to larger core charge densities and terminal voltages and currents (28). This type of measurement should help to resolve the questions regarding the efficacy of BTA and lead to a better understanding of the interfacial processes.

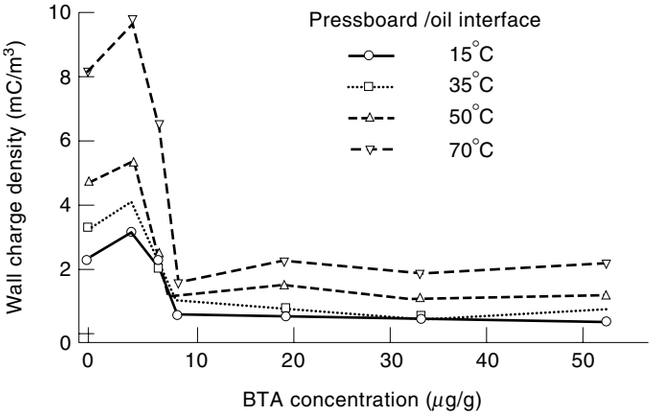

Figure 9. The wall charge density generally decreases once a critical concentration of 1,2,3-benzotriazole, in this case approximately 10 μg/g in transformer oil, is reached.

BIBLIOGRAPHY

1. K. B. Oldham and J. C. Myland, *Fundamentals of Electrochemical Science,* San Diego: Academic Press, 1994.
2. A. Klinkenberg and J. L. Van der Minne, *Electrostatics in the Petroleum Industry,* Amsterdam: Elsevier, 1958.
3. J. T. Leonard, Generation of electrostatic charge in fuel handling systems: A literature survey, *Naval Res. Lab. Rep. 8484,* September 1981.
4. J. T. Leonard and H. F. Bogardus, Pro-static agents in jet fuels, *Naval Res. Lab. Rep. 8021,* August 1976.
5. I. Ginsburgh, The static charge reducer, *J. Coll. Int. Sci.,* **32** (3): 424–432, 1970.
6. D. W. Crofts, The static electrification phenomena in power transformers, *IEEE Trans. Electr. Insul.,* **23**: 137–146, 1988.
7. R. Tamura et al., Static electrification by forced oil flow in large power transformers, *IEEE Trans. Power Appar. Syst.,* **9**: 335–343, 1980.
8. M. Yasuda et al., Suppression of static electrification of insulating oil for large power transformers, *IEEE Trans. Power Appar. Syst.,* **101**: 4272–4280, 1982.
9. S. Shimizu, H. Murata, and M. Honda, Electrostatics in power transformers, *IEEE Trans. Power Appar. Syst.,* **98**: 1244–1250, 1979.
10. M. Ieda et al., Suppression of static electrification of insulating oil for large power transformers, *IEEE Trans. Elec. Insul.,* **23** (1): 153–157, 1988.
11. J. C. Dean, G. M. Williams, and J. DeGiovanni, Analysis of flow electrification in fuel distribution systems, *IEEE Trans. Ind. Appl.,* **29**: 639–644, 1993.
12. P. Van Zant, *Microchip Fabrication: A Practical Guide to Semiconductor Processing,* New York: McGraw-Hill, 1997.
13. From troubleshooter to troublemaker, *IEEE Spectrum,* **25** (6): 14, 1988.
14. G. Touchard and H. Romat, Electrostatic charges convected by flow of dielectric liquid through pipes of different length and different radii, *J. Electrostatics,* **10**: 275–281, 1981.
15. G. Touchard et al., Flow electrification in power transformers—explanation of the wall current measurements, *IEEE Trans. Diel. Elec. Insul.,* **1** (4): 728–733, 1994.
16. B. Abedian and A. A. Sonin, Theory for electric charging in turbulent pipe flow, *J. Fluid Mech.,* **120**: 199–217, 1982.
17. B. Abedian and A. A. Sonin, Electric currents generated by turbulent flows of liquid hydrocarbons in smooth pipes: Experiment vs. theory, *Chem. Eng. Sci.,* **41** (12): 3183–3189, 1986.
18. H. L. Walmsley and G. Woodford, The generation of electric currents by the laminar flow of dielectric liquids, *J. Phys. D: Appl. Phys.,* **14**: 1761–1782, 1981.
19. H. L. Walmsley, The generation of electric currents by the turbulent flow of dielectric liquids: I. Long pipes, *J. Phys. D: Appl. Phys.,* **15**: 1907–1934, 1982.
20. H. L. Walmsley, The generation of electric currents by the turbulent flow of dielectric liquids: II. Pipes of finite length, *J. Phys. D: Appl. Phys.,* **16**: 553–572, 1983.
21. G. Touchard and S. Watanabe, Fluctuations of potentials induced by turbulent flows of dielectric liquids through metallic pipes, *IEEE Trans. Ind. Appl.,* **29**(3): 645–649, 1993.
22. S. M. Gasworth, J. R. Melcher, and M. Zahn, Electrification problems resulting from liquid dielectric flow, *EPRI Technical Report EL-4501,* 1986; S. M. Gasworth, *Electrification by liquid dielectric flow,* Ph.D. thesis, EECS Dept., MIT, 1985.
23. S. M. Gasworth, J. R. Melcher, and M. Zahn, Flow-induced charge accumulation in thin insulation tubes, *IEEE Trans. Electr. Insul.,* **23**: 103–115, 1988.
24. T. V. Oommen, Static electrification properties of transformer oil, *IEEE Trans. Electr. Insul.,* **23**: 123–128, 1988.
25. A. J. Morin II et al., An absolute charge sensor for fluid electrification measurements, *IEEE Trans. Electr. Insul.,* **26**: 181–199, 1991.
26. J. K. Nelson and M. J. Lee, Tandem-chamber charge density monitor, *IEEE Trans. Electr. Insul.,* **25**: 399–404, 1990.
27. A. J. Morin II, M. Zahn, and J. R. Melcher, Fluid electrification measurements of transformer pressboard/oil insulation in a Couette charger, *IEEE Trans. Electr. Insul.,* **26**: 870–901, 1991.
28. A. P. Washabaugh and M. Zahn, Flow electrification measurements of transformer insulation using a Couette flow facility, *IEEE Trans. Diel. Electr. Insul.,* **3**: 166–181, 1996.
29. A. P. Washabaugh and M. Zahn, A chemical reaction based boundary condition for flow electrification, *IEEE Trans. Diel. Electr. Insul.,* **4** (6): 688–709, 1997.
30. J. C. Gibbings, On the charging current and conductivity of dielectric liquids, *J. Electrostatics,* **19**: 115–119, 1987.
31. J. Gavis, Transport of electric charge in low dielectric constant fluids, *Chem. Eng. Sci.,* **19**: 237–252, 1964.
32. G. G. Touchard, T. W. Patzek, and C. J. Radke, A physicochemical explanation for flow electrification in low conductivity liquids, *Proc. 1994 IEEE Ind. Appl. Ann. Meet.,* **3**: 1669–1675, 1994.

ANDREW P. WASHABAUGH
Raychem Corporation
MARKUS ZAHN
Massachusetts Institute of Technology

STATIC MEMORIES. See SRAM CHIPS.